https://doi.org/10.20575/00000060
Polar Data Journal, Vol. 9, 14–29, April 2025

Spatiotemporally continuous temperature monitoring using optical fibers (Loop 2) for ground surface and subsurface with various vegetations on a flat area with slope surface in the internal Alaska from 2016 to 2019

Tadao INOUE [1], Kazuyuki SAITO [1]*, Go IWAHANA [2], Hiroki IKAWA [3], Hirohiko NAGANO [4] and Robert BUSEY [2]

[1] Japan Agency for Marine-Earth Science and Technology (JAMSTEC), 3173-25 Showa-machi, Kanazawa-ku, Yokohama, Kanagawa 236-0001.

[2] International Arctic Research Center, University of Alaska Fairbanks, 2160 Koyukuk Drive, Fairbanks, AK 99775-7340, USA.

[3] Hokkaido Agricultural Research Center, National Agriculture and Food Research Organization, 1 Hitsujigaoka, Toyohira, Sapporo, Hokkaido 062-8555.

[4] Institute of Science and Technology, Niigata University, 8050 Ikarashi 2 no-cho, Nishi-ku, Niigata, Niigata 950-2181.

*Corresponding author. Kazuyuki Saito (ksaito@jamstec.go.jp)

(Received September 11, 2024; Accepted February 5, 2025)

Abstract: We measured spatiotemporally continuous surface temperature using 5.4 km of fiber-optic cable with a distributed temperature sensing system at an observation site in interior Alaska. The study area is covered by diverse plant ecosystems in the Arctic region, including black spruce and open moss. The spatial and temporal resolutions were 0.5 m and 30 min, respectively. About 4.4 km of the cable was installed in a flat area at an elevation of approximately 210 m above sea level (a.s.l.), and the last 1 km section was installed along a slope facing northwest, with the highest point reaching approximately 410 m a.s.l. Four quadrats with different vegetation coverages were set in a flat area. The sensor cables ran along each side (approximately 30 m) and one diagonal of the square at the surface and at the depth of 0.2 m below the surface to measure the temperature variations in the active layers. The measurements spanned 985 days from July 13, 2016, to February 25, 2019, of which measurements were made on 893 days covering various seasons, including snow cover, snow melt, and warm weather.

1. Background & Summary

The Arctic region is considerably affected by global warming, with substantial increases in air temperature[1]. Large areas are underlain by permafrost with large amounts of carbon storage. Thawing of permafrost due to the rising air temperatures presents a serious concern of additional release of greenhouse gases. The active layer, which is the top-soil layer that undergoes seasonal freezing and thawing[2], acts as an important interface between the atmosphere and permafrost. In recent years, the thickness of the active layer has increased at many high-latitude sites[3]. Therefore, understanding the dynamics of the active layer, including its temperature, is important to understand the state of permafrost and is also necessary to investigate the response of the Arctic region to global warming.

Generally, active layer conditions are influenced by energy exchange through the ground surface and soil moisture content. Boreal forest areas in the Arctic region have diverse plant ecosystems that cover the ground surface. Canopy conditions, aerodynamic and radiative characteristics, and other factors that affect energy exchange and soil moisture vary greatly seasonally depending on the vegetation type and condition, snow cover, and other factors[4].

Earth System models, which are used for future projections of global warming, are unable to reproduce these characteristics due to the lack of observational data to improve these models, especially in terrestrial land schemes, leading to a high degree of uncertainty in model output[5].

The distributed temperature sensing (DTS) system used in this study is a temperature measurement device that exploits the temperature-dependent nature of the scattering property of optical fibers in certain wavelength bands and can measure spatiotemporally continuous temperatures along an optical fiber sensor cable.

We tested a prototype case (Loop 1) during 2012–2014 and 2015–2016[4, 6]. In this study (Loop 2), we used different fiber-optic cables than in the prototype Loop 1 case, installed over 5.4 km at the same interior Alaska site (Figure 1a) over an area of diverse vegetation cover (Figure 1b) spanning the flat and slope topography. The temperatures were continually recorded through the entire cable at 0.5 m and 30 min spatiotemporal resolution from July 2016 to February 2019.

While Loop 1 measured air and subsurface temperatures vertically at points with the fiber-optic cable coiled around PVC pipes, Loop 2 measured temperatures at surface and subsurface (at the depth of 20 cm) in 30 m square plots, referred to as "quadrats," installed at four locations of different vegetation types to evaluate statistical characteristics of temperature variations at surface and in the active layer across quadrats (Fig. 1b and 2a).

The cable sensor was further extended to cover the northwest-facing slope to evaluate the diurnal-to-seasonal development of the atmospheric boundary layer.

Although it is a single cable with a length of 5.4 km, the area where the cable was installed can be classified according to their characteristics relating to spatial locations and vertical positions (i.e. surface and subsurface), so for convenience, we have conceptually divided the cable into segments and given a name to each segment (e.g., A_u01) which are indicated in Figures 2 and 3, and these names were also given to all data points as "Segment Name" in the observation point-location information file (Section 4, 1 (2) and Table 2).

2. Study Location

The observations were made at the Poker Flat Research Range (PFRR; 147.487 W, 65.123N), located 50 km northeast of Fairbanks in the interior of Alaska, USA (Fig. 1a). The facility is managed by the Geophysical Institute of the University of Alaska, Fairbanks. Because it is located in a discontinuous permafrost zone, permafrost partially underlies the observation site.

3. Methods

The DTS system was installed to continuously measure the temperature in space and time using the principle of light scattering and the physical properties of fiber-optic cables. This method is referred to as optical time-domain reflectometry (OTDR)[7]. The system consists of a control unit that emits laser pulses and receives reflected waves, and a fiber-optic cable connected to the control unit.

In the backscattering phenomena of a laser pulse emitted from the control unit at a molecule in the optical fiber, Raman scattering produces two distinct components: the Stokes component at a higher frequency and the anti-Stokes component at a lower frequency than the Rayleigh scattering. As the former has a low temperature dependence, and the latter has a high temperature dependence, the temperature of the molecules at each point of the cable is estimated from the ratio of the two[4]. The distance between the observation point and the controller was obtained from the reflection time of the laser pulse[4, 6, 7, 8] (cf. Figure 2 in Saito *et al.* 2023).

We used a DTS (model number: N4386B) manufactured by AP Sensing as the control unit. The optical fiber cable is a dual-core type (multi-mode, GI50/125, outer ϕ 4.0 mm, Armored FO Cable), manufactured by Kaiphone Communication (Taiwan/China). The operating temperature range of the cable is -40°C to 85°C.

Two ends of the optical fibers in the cable on the control unit side were connected to channels 3 and 4 of the device, respectively, whereas the farthest opposite ends of separated two optical fibers in the dual-core optical fiber cable were connected to each other to form a single optical fiber (Fig. 2a). Laser pulses were alternately emitted from each channel at 5-second interval to measure the values at the same point from two directions. The temperature at each observation point was calculated from these two values as a 30-minute average.

The software "DTS Configurator" was provided by AP Sensing as a set with the control unit and runs on Microsoft Windows 7. The temperature, the original DTS signal, and the signal loss were recorded in text format.

The spatial resolution was set to 0.5 m and the temporal resolution to 30 min. The total length of the dual-core optical fiber cable was approximately 5.4 km.

The fiber-optic cable was laid on the ground surface in areas of various vegetation coverage at the PFRR site (Fig. 1b). A 30 m square (and one diagonal line), which we call "quadrat," were set at four representative vegetation areas in a flat section of an elevation of approximately 210 m a.s.l. The areas were selected at the sight by visual inspection of relative contrast and dominance of covering vegetation types and labeled as:

Quadrat A: Sparse conifers/mosses

Quadrat B: Dense conifers

Quadrat C: Open Moss

Quadrat D: Deciduous/mixed

Note that the dominant numbers of satellite-based vegetation classes within each quadrat, provided in the locational information file (Section 4, 1 (2) and Table 2), do not necessarily agree with these labels.

Simultaneously, the fiber-optic cable was laid at a depth of 0.2 m with a horizontal configuration similar to that on the ground surface (Fig. 2b–e). This enabled us to obtain spatially representative temperatures and their statistical spatiotemporal variations at the surface and shallow subsurface of the same vegetation area (Fig. 3). The last kilometer of the cable was installed on a northwest-facing slope section with a maximum elevation of approximately 410 m a.s.l.

Measurements were taken from July 13, 2016, to February 25, 2019 (893 observation days). The days without data for the entire period are listed below.

2016-08-12~2016-09-02, 2016-09-21~2016-09-29, 2016-11-02~2016-11-03, 2017-03-22~2017-04-11, 2017-08-08, 2017-08-26, 2017-09-13~2017-09-14, 2017-09-16~2017-09-18, 2017-09-20, 2018-12-18~2018-12-19, 2019-02-11, 2019-02-19

The suspicious measurements were found between October 8, 2018, and November 9, 2018. The temperature data of this period showed occasional anomalous fluctuations, with the values ranging from approximately -10°C to 30°C, even in the subsurface sections. We retained the data taken during the period in the dataset, however, use of this portion of the data is not recommended.

A 16-meter-high flux observation tower, installed near the control unit, measured air temperature (30-minute average) 1.5 m above the ground using a ventilated thermometer (Vaisala HMP155), which was used for quality control of the DTS temperature data for the segment FL (Fig. 4a–c). The observation tower was constructed in 2010 as part of a collaborative study under the JAMSTEC-IARC Collaboration Study (JICS) between the Japan Agency for Marine-Earth Science and Technology (JAMSTEC) and UAF's International Arctic Research Center (IARC). Ground temperatures measured by a thermistor sensor (HOBO TMC6-HE with HOBO UX120-006M data logger) were used to validate the subsurface portion of the DTS data. This single point measurement was installed at the depth of 0.17 m in Quadrat A (Fig. 4d–f). The measurement period matched with that of the DTS data.

Land surface vegetation types (Fig. 1b) were classified into eight categories using a supervised classification method (Maximum Likelihood algorithm) based on WorldView-2 high-resolution multispectral imagery (spatial resolution of 2 m; observation date: June 5, 2017). The index numbers and categories were as follows:

0: Water

1: Developed

2: Barren / Grass

3: Deciduous / Mixed

4: Dense Conifer

5: Sparse Conifer

6: Sparse Conifer / Moss

7: Open Moss

Here, “conifer” refers primarily to black spruce[9].

“Mixed” refers to mixed forests of conifers and deciduous broadleaf trees.

The segments in the quadrats were flagged to distinguish between the ground surface and subsurface because some of the segments were buried in the subsurface. Zero and one indicate the ground surface and subsurface, respectively, in an observation point-location information file (Section 4, 1 (2) and Table 2).

4. Data Records

Quality controlled temperature data is provided as ASCII files and binary data (#2). Two sets of attribute data are provided in a comma-separated value (csv) text file format (#1).

The first (#1 (1)) is the temporal information file for each observation record, in which each line corresponds to a temperature measurement point.

The second (#1 (2)) is for the Loop 2 DTS observation location, which describes the spatial information of each observation point at 0.5 m intervals, including the point number, longitude, latitude, vegetation type index, elevation, and segment name, which were derived from integrating analyses employing the GPS survey results along the cable and satellite observations.

1. Attribution files.

(1) Temporal information (1 file).

A comma-separated value (csv) text file with entities of [Data Number, Year, Month, Day, Hour, Minute, Date, Day of Year] (Table 1), where Year, Month, Day, Hour, Minute are in Alaska Standard Time (AKST; UTC - 9 h); “Date” is the elapsed day starting at 0:00 a.m. on the 1st of January 2016, AKST, to the nearest fraction of a day; “Day of Year” is the elapsed day starting at 0:00 a.m., January 1 of each year, expressed as a fraction of a day.

The number of stored items is 41449 items.

The file name is DTS_temporal_info_v1.csv.

(2) Observation point-location information (1 file)

A comma-separated-value (csv) text file containing location information for each observation point at 0.5 m intervals in the DTS, arranged in the order [point number, longitude, latitude, vegetation type index, elevation, segment name, ground surface and subsurface classification index], containing 10831 items. The point number starts with 94, which is the starting point for substantive observations (starting point of quadrat A). The longitude and latitude of each point were interpolated from the GPS logger observations along the installed fiber-optic cable. The vegetation types were classified into eight categories.

The segment names were used for convenience when classifying the location of the DTS. The first letters A through D denote quadrat numbers, and [A–D]_u and [A–D]_g indicate the valid subsurface and ground surface segments in the quadrats, respectively (Fig. 2 and 3). The others (A-B, B-P, P-C, C-D, FL, and SL) were located between and outside the quadrats.

The file name is DTS_spatial_info_v1.csv.

2. Quality-controlled temperature data files (41449 files)

ASCII files (ASCII) for each period in DTS_temporal_info_v1.csv listing the temperature data (in °C) according to the order in DTS_spatial_info_v1.csv are the core of the data. The files were organized into folders by year and month. The number of files per year is as follows:

2016: 6384 files

2017: 15925 files

2018: 16848 files

2019: 2292 files

These files can be read with a text editor and opened using a spreadsheet software such as Microsoft Excel.

The file-naming convention was PFRR_Loop2_DTS_YYYYMMDD_HHMN.csv, where YYYY, MM, DD, HH, and MN denote the year, month, day, hour, and minute of the record in ASCII, respectively.

Example of the data (PFRR_Loop2_DTS_20160731_1206. csv):

```
4.93109703063965
4.04179191589355
3.39791679382324
4.22815465927124
2.65605258941650
2.02893257141113
2.71824932098389
3.28388929367065
4.77527856826782
4.35039663314819
```

(omission)

14.65712356567380
14.09741687774660
15.49048995971680
15.08106040954590
10.85245227813720
7.56110095977783
5.34277677536011
4.92793512344360
3.68657207489014
3.50245857238770
(omission)
11.75385093688960
12.63011741638180
12.26495456695560
11.68311405181880
11.65850257873540
11.89793395996090

We also prepared 8-byte binary (little-endian) data, which is a compilation of the csv files. This can be used to compile specific time data using the separately provided Fortran program ("read_Loop2_Tracedata_fromBinary_v1.f90" has been tested with gfortran; the bash script "run_read_Loop2_Tracedata_fromBinary_v1.sh ", which can be used to extract data at a specific time, is also included). gfortran is a free software and can be obtained from the GNU Gfortran site (https://gcc.gnu.org/wiki/GFortran).

5. Technical Validation

(1) Temperature calibration in the control unit was performed at the beginning of the measurements (see 5. Technical Validation #1 in Saito *et al.*, 2023).

(2) Comparison with other temperature measurements

The temperatures for each time step (every 30 min) for segment FL (the 1335.5 m long latter half of the flat area after Quadrat D; data numbers 6491–9161; Fig. 2a) were analyzed for the mean, maximum, and minimum temperatures of each day. These values were compared with the corresponding daily mean, maximum, and minimum temperatures observed at the tower (air temperatures at 1.5 m height), respectively. For the range above 0°C, the DTS temperatures have a very good correlation with the air temperatures of tower data; below 0°C, the DTS temperatures show higher values presumably due to the insulating effect of snow cover, although the difference with the tower data is within the reasonable range (Fig. 4a–c).

Whereas single point thermistor measurements of ground temperature at 0.17 m depth in Quadrat A were compared with the DTS data of each time step for spatially averaged temperatures of segments A_u, that is, six subsurface segments in Quadrat A (Fig. 2b). They are well correlated for the entire temperature range, and the coefficients of determination (r^2) for mean, maximum, and minimum values are 0.92, 0.92, and 0.90, respectively (Fig. 4d–f).

In the validations, the DTS measurements of the anomalous fluctuation period, which is indicated in Section 3 (Methods), were not used. Similarly, the outliers of thermistor-based ground temperature measurements were identified by the Grubbs test[10] (two-sided at the 0.05 significance level) and removed.

(3) Anomalous values removed

In the measurement with the dual-core cable, where the inner two optical fibers are connected at the end of the cable, data can be obtained twice the length of the laid fiber-optic cable (round trip = 10.8 km worth); however, because of the nature of noise that increases with the distance from the laser emission channel, only the first half of the data (approximately 5.4 km worth), which was closer to the laser emission channel, was used (Fig. 3a, b).

6. Usage Notes

It should be noted that the latitude and longitude assigned to each observation point at 0.5 m intervals were not directly measured for each point but were interpolated for each point from the latitude and longitude of the sample measurements taken by the GPS loggers.

Basically, the data are collected every 30 min, but there may be cases where the data are not precisely on the hour or 30 min owing to a reset of the control unit or other reasons, or there may be only one data point per hour.

The preliminary summary data of the Loop 2 measurement published through the Arctic Data archive System (ADS data: https://ads.nipr.ac.jp/dataset/A20191021-002) contained the values by each point averaged on the monthly and annual basis from July 2016 to January 2019. However, the dataset lacked the spatial attribution information of the points such as longitude, latitude, vegetation cover type, and cable segments. Therefore, we carried out the overall renewal of the data editing to produce this comprehensive dataset (ADS data: https://ads.nipr.ac.jp/dataset/A20240412-002). The attributional information was assigned for each DTS observation point with longitude, latitude, altitude, vegetation index, subsurface index, and revised segment determination. The raw data were quality-controlled rigorously. Note that the attribution files introduced in this paper can only be applicable to the new data set (A20240412-002).

7. Competing interests

The authors have no competing interests to declare.

8. Figures

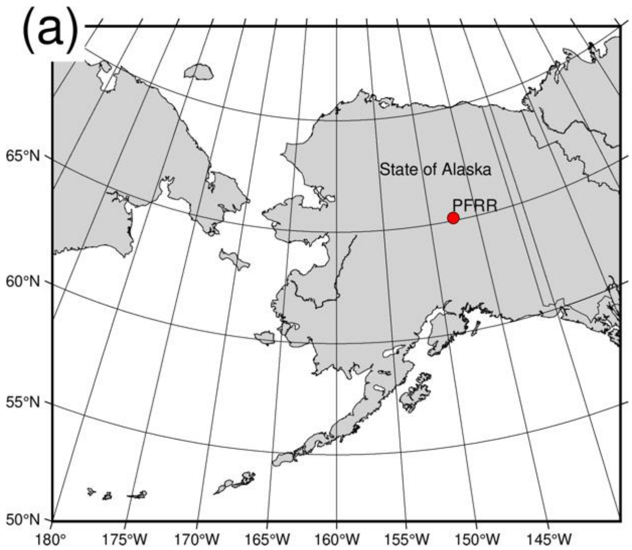

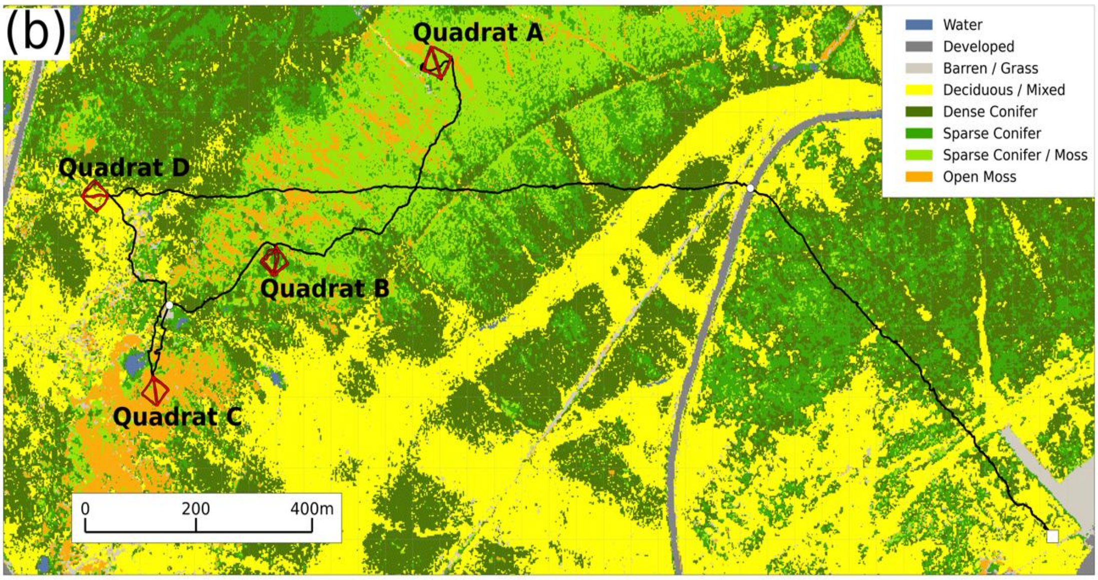

Figure 1. (a) Location of the observation site. (b) Layout of the fiber-optic cable sensor with surface vegetation types. The red lines, two white circles, a white square indicate quadrats, border of long-range segments, and end of the fiber-optic cable, respectively and they correspond with the same symbols in Fig. 2(a).

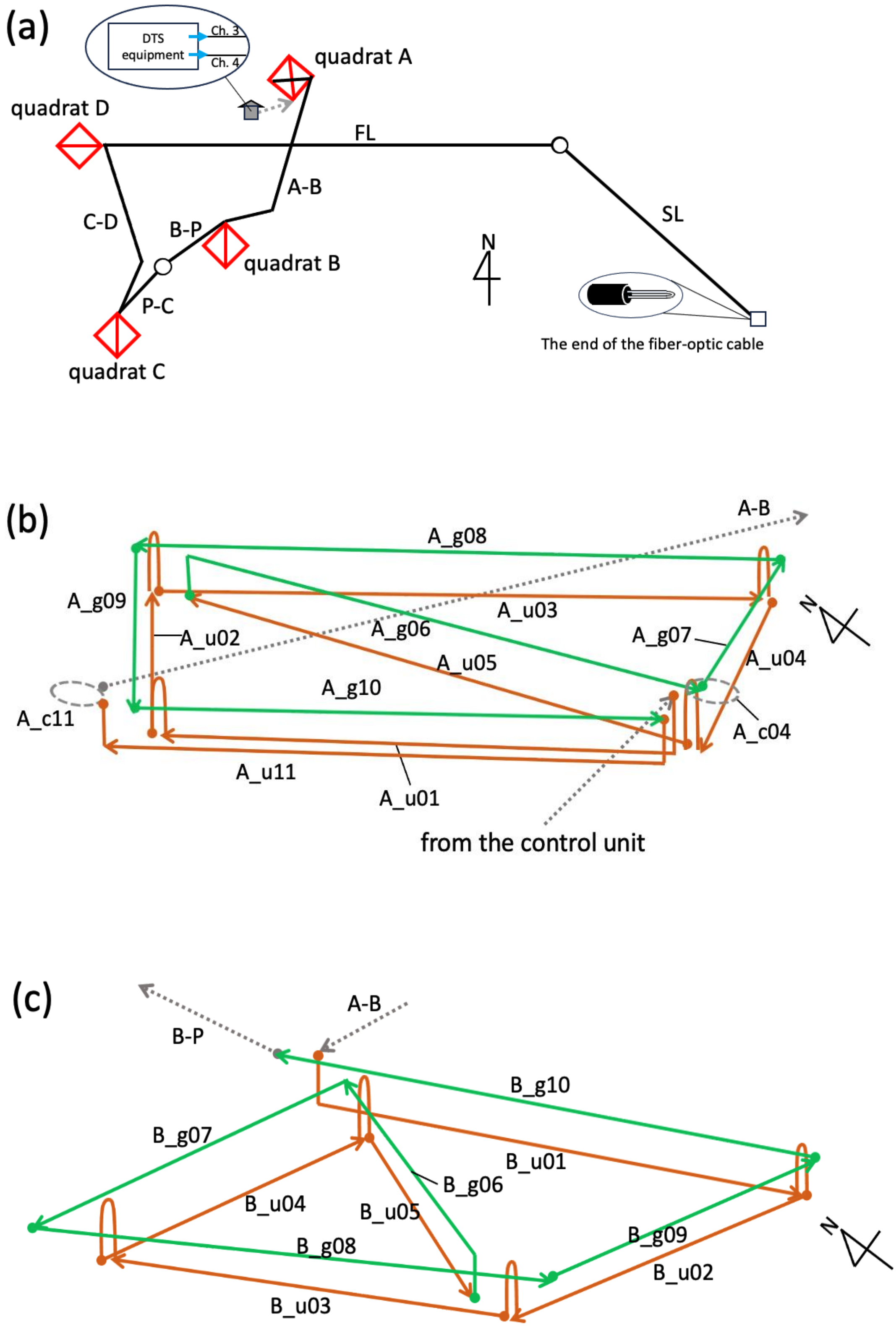
(a)
DTS equipment
Ch. 3
Ch. 4
quadrat A
quadrat D
FL
A-B
C-D
B-P
quadrat B
SL
N
P-C
quadrat C
The end of the fiber-optic cable
(b)
A-B
A_g08
A_g09
A_u03
A_u02
A_g06
A_g07
A_u04
A_u05
A_g10
A_c11
A_c04
A_u11
A_u01
from the control unit
(c)
A-B
B-P
B_g10
B_g07
B_u01
B_g06
B_u04
B_u05
B_g08
B_g09
B_u03
B_u02

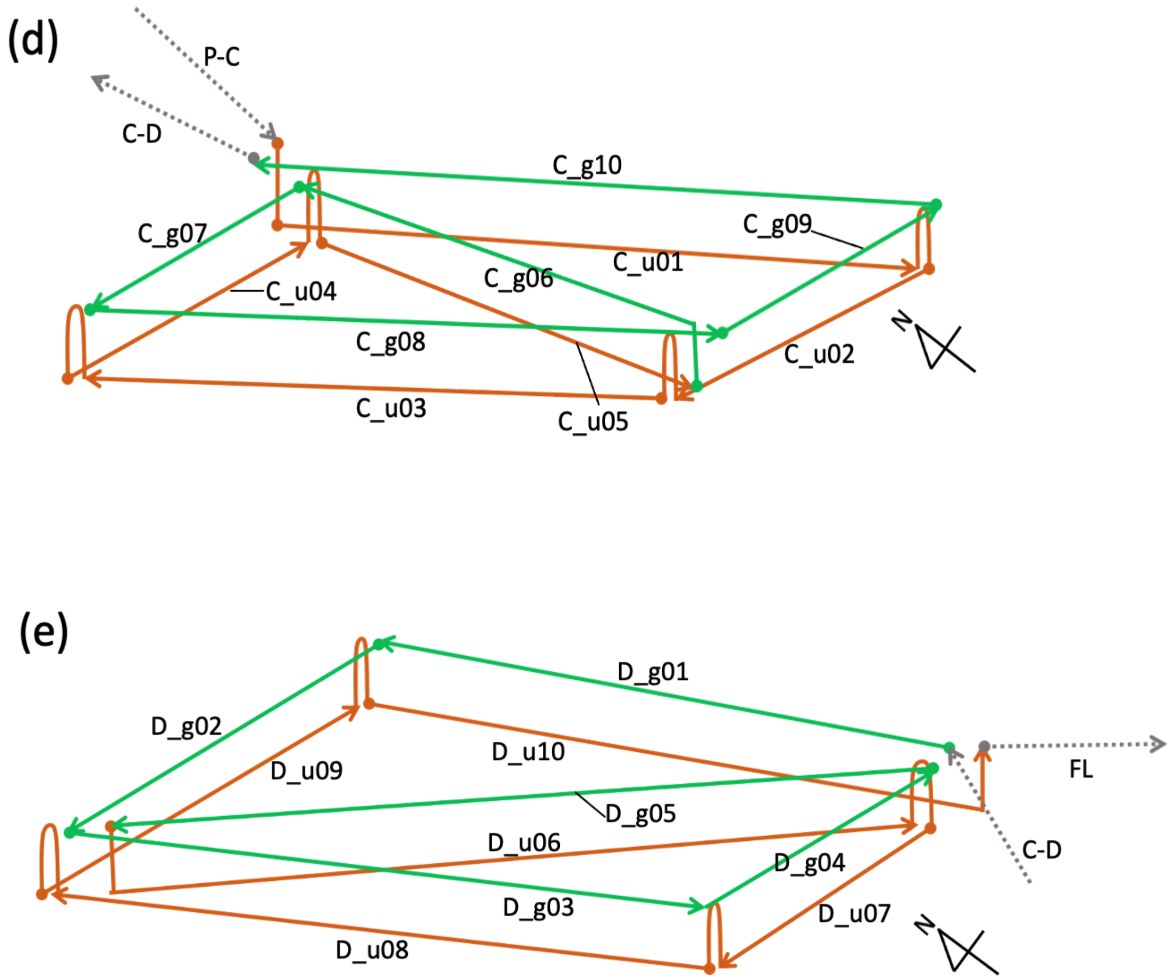

Figure 2: (a) Schematic diagram of Loop 2. (b) Schematic diagram of Quadrat A. (c) Schematic diagram of Quadrat B. (d) Schematic diagram of Quadrat C. (e) Schematic diagram of Quadrat D. The green and orange lines indicate surface and subsurface segments, respectively. Quadrats are special areas where the fiber-optic cable was installed both on the surface and 0.2 m under the ground (i.e., subsurface) to detect the temperatures in the active layer. A quadrat was set up in a square shape with each of four sides approximately 30 m long and one diagonal line. The single cable of 5.4 km long was conceptually divided into segments according to their characteristics relating to spatial locations and vertical positions (i.e., surface and subsurface) for convenience and given a name for each segment (e.g., A_u01).

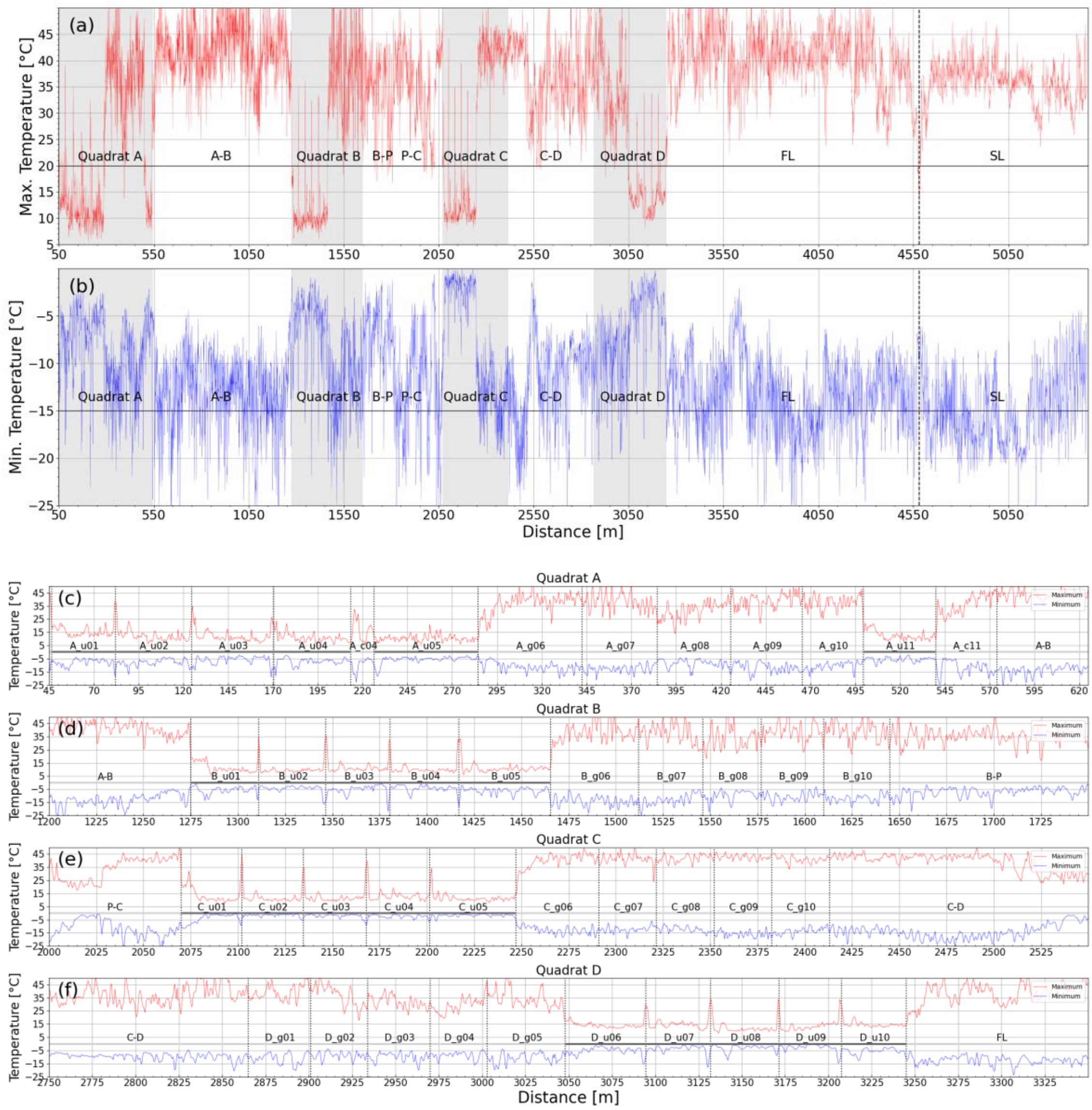

Figure 3. Maximum and minimum temperatures at each DTS point between October 2017 and September 2018. The red and blue lines indicate maximum and minimum temperatures, respectively. (a) and (b) show maximum and minimum temperatures in the entire Loop2 area, respectively. The shaded areas indicate the quadrat zone. (c) to (f) indicate enlarged quadrat A to D area, respectively.

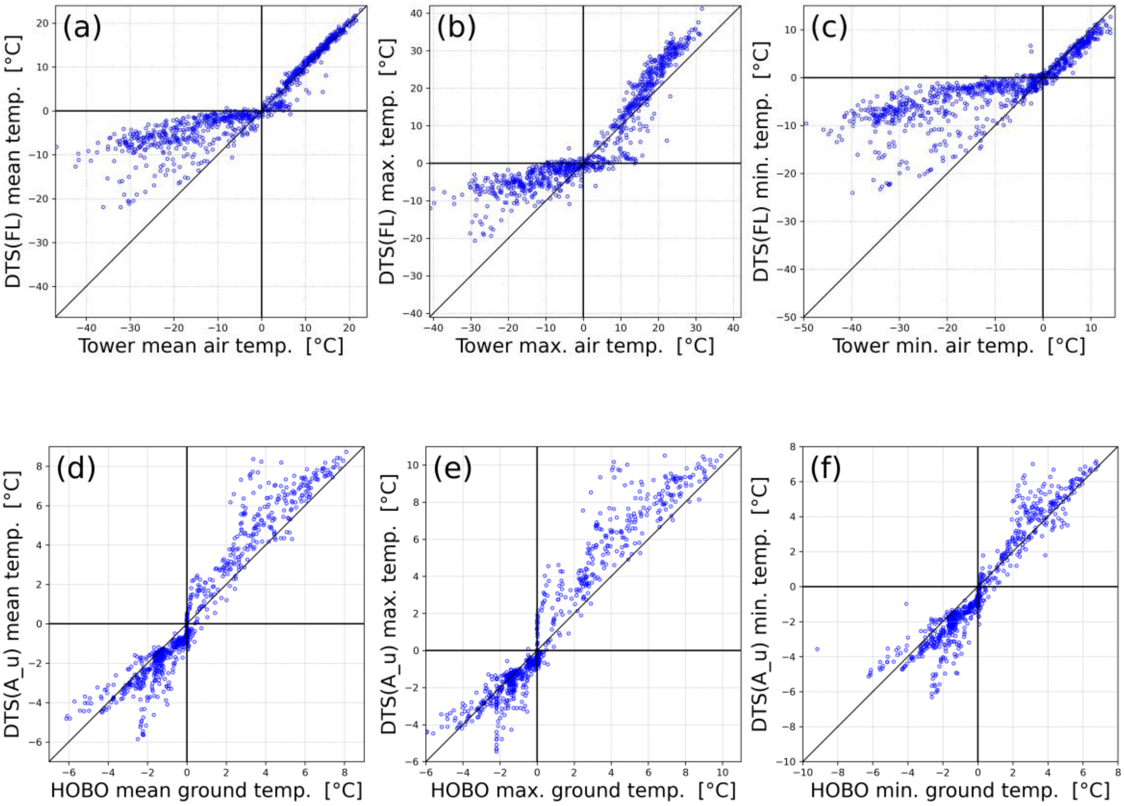

Figure 4. Respective correlation between tower-observed air temperatures at 1.5 m and DTS temperatures within the segment FL for daily (a) mean, (b) maximum, and (c) minimum temperatures for the observed period. (d), (e), and (f) are the same as (a), (b), and (c) except for correlations between the HOBO thermistor-observed ground temperature at a depth of 0.17 m and DTS temperatures of the subsurface segments in Quadrat A (e.g., A_u).

9. Tables

Table 1. The data structure of the temporal information file.

Data Number	Year	Month	Day	Hour	Minute	Day from 1st January 2016	Day of Year
0	2016	7	13	17	0	194.708333	194.708333
1	2016	7	13	17	30	194.729167	194.729167
2	2016	7	13	18	0	194.750000	194.750000
3	2016	7	13	18	30	194.770833	194.770833
4	2016	7	13	19	0	194.791667	194.791667
5	2016	7	13	19	30	194.812500	194.812500
6	2016	7	13	20	0	194.833333	194.833333

(omission)

6383	2016	12	31	23	34	365.981944	365.981944
6384	2017	1	1	0	4	366.002778	0.002778
6385	2017	1	1	0	34	366.023611	0.023611
6386	2017	1	1	1	4	366.044444	0.044444
6387	2017	1	1	1	34	366.065278	0.065278
6388	2017	1	1	2	4	366.086111	0.086111
6389	2017	1	1	2	34	366.106944	0.106944
6390	2017	1	1	3	4	366.127778	0.127778

Table 2. The data structure of the locational information file.

Data Number	Longitude	Latitude	Vegetation Type	Altitude	Segment Name	Subsurface Index
94	-147.486965	65.123461	6	210.18	A_u01	1
95	-147.4869608	65.12346518	6	210.24	A_u01	1
96	-147.4869566	65.12346936	6	210.24	A_u01	1
97	-147.4869595	65.12347354	6	210.24	A_u01	1
98	-147.4869637	65.12347772	6	210.23	A_u01	1
99	-147.4869714	65.12348064	6	210.23	A_u01	1
100	-147.4869806	65.123483	6	210.17	A_u01	1
101	-147.4869898	65.12348536	6	210.17	A_u01	1
102	-147.486999	65.12348772	6	210.17	A_u01	1

Author contributions

T. Inoue edited the data, checked the data quality, produced programming codes for editing and visualizing the data, and wrote an early draft of the manuscript. K. Saito initiated, designed, and supervised the entire project; procured sets of equipment; negotiated the use of PFRR; led the deployment of the cable sensor; and performed calibrations, programming, and measurements of the DTS system. G. Iwahana and R. Busey contributed to installing the DTS equipment. GI, H. Nagano, and H. Ikawa contributed to maintaining DTS measurements. GI conducted land cover classification for the site and generated geographical information figures. The RB supervised the technical aspects of the project. All authors contributed to the final manuscript with input, suggestions, and editing.

Acknowledgements

This project was conducted as a part of the JAMSTEC (Japan Agency for Marine-Earth Science and Technology) and IARC (International Arctic Research Center, University of Alaska, Fairbanks) Collaboration Study (JICS), and in part supported by the Integrated Research Program for Advancing Climate Models (TOUGOU Program, JPMXD0717935715), the Advanced Studies of Climate Change Projection (SENTAN Program, JPMXD0722681344), the Arctic Challenge for Sustainability (ArCS, JPMXD1300000000), and the Arctic Challenge for Sustainability II (ArCS II, JPMXD1420318865). The authors are grateful to Mr. Naoki Kukuu, Mr. Ryota Kajita, Dr. Yasunori Igarashi, Dr. Yoshinobu Harazono, and Mr. Yusuke Futakuchi for their cooperation and support in the installation of the sensor cables, Mr. Masataro Ishiguro for his preliminary analysis for statistical summarization (https://ads.nipr.ac.jp/dataset/A20191021-002) and GIS analysis to segment the cable, Dr. Hideki Kobayashi for his management of the JICS site, and Dr. Kathe Rich and Mr. Robert Valdez for their cooperation and facilitation in investigating the PFRR site.

References

1. Serreze, M. C. et al. Observational Evidence of Recent Change in the Northern High-Latitude Environment. Climatic Change. 2000, 46, p. 159–207. https://doi.org/10.1023/A:1005504031923.
2. Burn, C. R. The active layer : two contrasting definitions. Permafrost and Periglacial Processes. 1998, 9 (4), p. 411–416. https://doi.org/10.1002/(SICI)1099-1530(199810/12)9:4<411::AID-PPP292>3.0.CO;2-6.
3. IPCC, 2021. Climate Change 2021: The Physical Science Basis. Contribution of Working Group I to the Sixth Assessment Report of the Intergovernmental Panel on Climate Change [Masson-Delmotte, V. et al. (Eds.)]. Cambridge University Press. 2021, 2391 p. https://doi.org/10.1017/9781009157896.
4. Saito, K.,Iwahana, G., Ikawa, H., Nagano, H., and Busey, R. Spatiotemporally continuous temperature monitoring using optical fibers (Loop1) in the internal forest areas in Alaska for the period from 2015 to 2016. Polar Data Journal. 2023, 7, p. 58–71. https://doi.org/10.20575/00000049.
5. Yokohata et al. Model improvement and future projection of permafrost processes in a global land surface model. Progress in Earth and Planetary Science. 2020, 7 (69). https://doi.org/10.1186/s40645-020-00380-w.
6. Saito, K., Iwahana, G., Ikawa, H., Nagano, H., and Busey, R. C. Links between annual surface temperature variation and land cover heterogeneity for a boreal forest as characterized by continuous, fibre-optic DTS monitoring, Geoscientific Instrumentation, Methods and Data Systems. 2018, 7 (3), p. 223–234. https://doi.org/10.5194/gi-7-223-2018.
7. Dakin, J. P., Pratt, D. J., Bibby, G.W., and Ross, J. N. Distributed optical fibre Raman temperature sensor using a semiconductor light source and detector. Electronics Letters. 1985, 21 (13), p. 569–570. https://doi.org/10.1049/el:19850402.

8. Vogt, T., Schneider, P., Hahn-Woernle, L., and Cirpka, O. A. Estimation of seepage rates in a losing stream by means of fiber-optic high-resolution vertical temperature profiling. Journal of Hydrology. 2010, 380 (1–2), p. 154–164. https://doi.org/10.1016/j.jhydrol.2009.10.033.
9. Nakai, T. et al. Characteristics of evapotranspiration from a permafrost black spruce forest in interior Alaska. Polar Science. 2013, 7 (2), p. 136–148. https://doi.org/10.1016/j.polar.2013.03.003.
10. Grubbs, F. E. Procedures for Detecting Outlying Observations in Samples. Technometrics. 1969, 11 (1), p. 1–21. https://doi.org/10.2307/1266761.

Data Citations

Saito, K., Iwahana, G., Ikawa, H., Nagano, H., Busey, R., and Inoue, T. Spatiotemporally continuous temperature monitoring using optical fibers (Loop2) in the ground surface and subsurface for the various forest areas, open areas, and the slope in Alaska from 2016 to 2019. 1.00, Japan, Arctic Data archive System (ADS), 2025. https://doi.org/10.17592/001.2024041202.